Title
Rbfox Proteins Regulate Splicing as Part of a Large Multiprotein Complex LASR

Journal
Cell, 165(3)

ISSN
0092-8674

Authors
Damianov, Andrey
Ying, Yi
Lin, Chia-Ho
et al.

Publication Date
2016-04-01

DOI
10.1016/j.cell.2016.03.040

Peer reviewed

Published in final edited form as:

Cell. 2016 April 21; 165(3): 606–619. doi:10.1016/j.cell.2016.03.040.

Rbfox proteins regulate splicing as part of a large multiprotein complex LASR

Andrey Damianov[1], **Yi Ying**[2], **Chia-Ho Lin**[1], **Ji-Ann Lee**[3], **Diana Tran**[1], **Ajay A. Vashisht**[3], **Emad Bahrami-Samani**[1], **Yi Xing**[1], **Kelsey C. Martin**[3], **James A. Wohlschlegel**[3], and **Douglas L. Black**[1,*]

[1]Department of Microbiology, Immunology, and Molecular Genetics, University of California, Los Angeles, Los Angeles, CA 90095, USA

[2]Molecular Biology Interdepartmental Ph.D. Program, University of California, Los Angeles, Los Angeles, CA 90095, USA

[3]Department of Biological Chemistry, University of California, Los Angeles, Los Angeles, CA 90095, USA

Summary

Rbfox proteins control alternative splicing and posttranscriptional regulation in mammalian brain, and are implicated in neurological disease. These proteins recognize the RNA sequence (U)GCAUG, but their structures and diverse roles imply a variety of protein-protein interactions. We find that nuclear Rbfox proteins are bound within a large assembly of splicing regulators (LASR), a multimeric complex containing the proteins hnRNP M, hnRNP H, hnRNP C, Matrin3, NF110/NFAR-2, NF45, and DDX5, all approximately equimolar to Rbfox. We show that splicing repression mediated by hnRNP M is stimulated by Rbfox. Virtually all the intron-bound Rbfox is associated with LASR, and hnRNP M motifs are enriched adjacent to Rbfox crosslinking sites *in vivo*. These findings demonstrate that Rbfox proteins bind RNA with a defined set of cofactors, and affect a broader set of exons than previously recognized. The function of this multimeric LASR complex has implications for deciphering the regulatory codes controlling splicing networks.

Introduction

Patterns of alternative pre-mRNA splicing are controlled by specialized proteins that assemble onto the pre-mRNA and control splice site choices (Fu and Ares, 2014; Lee and

*Corresponding author, DougB@microbio.ucla.edu. .

Author Contributions

Conceptualization, AD and DLB; Methodology, AD, YY, and DLB; Investigation, AD, YY, JAL, DT and AAV; Software, EBS and YX; Formal Analysis, CHL and EBS; Data Curation, CHL; Writing – Original Draft, AD and DLB; Writing – Review and Editing, AD, YY, JAL, YX, KCM, and DLB; Supervision, AD, YX, JAW, KCM and DLB; Project Administration, KCM and DLB; Funding Acquisition, YX, KCM, JAW and DLB.

Rio, 2015). The Rbfox family of splicing regulators includes three mammalian paralogs Rbfox1 (A2BP1), Rbfox2 (RBM9), and Rbfox3 (NeuN) that are all expressed in neurons and can show specific expression in other cell types (Kuroyanagi, 2009).

Rbfox proteins affect a wide range of synaptic and neurodevelopmental functions. Conditional Rbfox1 deletion in the mouse brain leads to a seizure phenotype, while mice without brain Rbfox2 exhibit cerebellar defects and ataxia (Gehman et al., 2012; Gehman et al., 2011). Mutations in Rbfox1 and Rbfox3 are found in human epilepsy patients (Bhalla et al., 2004; Lal et al., 2013a; Lal et al., 2013b), while other findings connect Rbfox1 with autism spectrum disorders and spinocerebellar ataxias (Bill et al., 2013). Rbfox2 is also upregulated in certain cancers and controls exons during the epithelial-mesenchymal transition (Braeutigam et al., 2014; Venables et al., 2013). These findings have led to substantial clinical interest in Rbfox protein function.

The Rbfox proteins all contain a single highly conserved RNA recognition motif (RRM) that specifically binds the sequences UGCAUG and GCAUG (Auweter et al., 2006; Jin et al., 2003; Lambert et al., 2014). Alternative promoters and alternative splicing produce multiple protein isoforms from each Rbfox locus, with varying subcellular localization and splicing activity (Damianov and Black, 2010; Lee et al., 2009; Nakahata and Kawamoto, 2005). In addition to controlling splicing patterns, cytoplasmic Rbfox isoforms bind to 3′ UTR targets to affect downstream gene expression (Lee et al., 2016). Target transcripts for both nuclear and cytoplasmic proteins encode many proteins essential to neuronal development and synaptic activity (Gehman et al., 2012; Gehman et al., 2011; Lee et al., 2016; Lovci et al., 2013; Weyn-Vanhentenryck et al., 2014).

Typically, binding of Rbfox to a (U)GCAUG element downstream of the alternative exon promotes its splicing, whereas binding to an upstream element, or an element within the exon, represses exon inclusion (Jangi et al., 2014; Lovci et al., 2013; Tang et al., 2009; Weyn-Vanhentenryck et al., 2014; Yeo et al., 2009; Zhang et al., 2008). However, many (U)GCAUG elements proximal to alternative exons do not affect splicing or exhibit Rbfox binding. Conversely, (U)GCAUG elements located more than 500 nucleotides away from a target exon can function through base-pairing interactions that bring the bound protein closer to the exon (Lovci et al., 2013). Moreover, some Rbfox binding sites identified in genomewide assays do not encompass a (U)GCAUG element. Thus, the features determining whether and how Rbfox will affect splicing are not understood.

We find that nuclear Rbfox proteins function within a large macromolecular complex containing a distinct set of other splicing factors that affect the recruitment of Rbfox to its targets.

Results

Rbfox proteins engage in distinct protein and RNA interactions in different nuclear compartments

To examine the portion of Rbfox protein engaged with nascent RNA, we isolated nuclei from brain tissue followed by lysis in Triton X-100. The majority of Rbfox proteins pelleted

with chromatin and other high molecular weight (HMW) material, with less than 10% of the protein present in the soluble nuclear fraction (Fig. 1AB). Rbfox proteins could be extracted from the pellet fraction using RNase, and more efficiently with Benzonase nuclease that cleaves both RNA and DNA (Fig. 1AB), and which removed more than 99% of the bulk RNA from the fraction. We used this method to prepare subnuclear extracts from both mouse brain and cultured cells. Note that this extraction differs from methods to isolate nascent RNA, in which the chromatin is pelleted in high salt and urea to eliminate many intermolecular interactions while maintaining RNA polymerase association with DNA and nascent RNA (Khodor et al., 2011; Pandya-Jones and Black, 2009; Wuarin and Schibler, 1994). Our intent was to preserve protein-protein interactions while eliminating interactions mediated by RNA. The pellet fraction contains high molecular weight material that is spun down with chromatin, but is not necessarily in direct interaction with it. The release upon nuclease treatment indicates that a large portion of Rbfox protein is associated with RNA (see below).

Different types of splicing regulators exhibited different partitioning between the HMW fraction and the soluble nucleoplasm (Fig. 1B and S1). Similar to Rbfox, the majority of hnRNPs A1, A2/B1 and Q/R, as well as the SR proteins, were found in the HMW pellet and released with nuclease (Fig. 1B and S1, in Fig. S1 compare the input lanes). These proteins are enriched in nuclear speckles, indicating that nuclear speckle material also pelleted with the HMW fraction (Misteli et al., 1998; Tripathi et al., 2012). Unlike Rbfox, splicing factors such as PTBP2 and hnRNP K showed approximately equal distribution between the HMW and soluble fractions. Other proteins such as Nova were enriched in the soluble nuclear fraction (Fig. 1B and S1).

To examine Rbfox/RNA interactions in these two nuclear compartments, we performed individual nucleotide resolution crosslinking immunoprecipitation (iCLIP) on fractions of adult mouse brain (König et al., 2010). UV-irradiation of triturated brain tissue did not alter the location of the Rbfox proteins (Fig. S2A). *In vivo* crosslinking data was generated for Rbfox1, Rbfox2, and Rbfox3 in the HMW fractions of adult mouse forebrain and hindbrain, and for Rbfox1 in the soluble nuclear fraction of these regions. Crosslinked Rbfox1, 2 and 3 were also isolated from the soluble nuclear fraction of whole mouse brain (Table S1A). Crosslinked sequences were aligned to the mouse genome and significant clusters of iCLIP tags were defined (König et al., 2010). Crosslinking commonly generates an iCLIP tag terminating one nucleotide downstream. This position was frequently, but not always within a (U)GCAUG element (see below). The identified clusters overlapped with previous maps of Rbfox binding from unfractionated brain tissue (Lovci et al., 2013; Weyn-Vanhentenryck et al., 2014, Fig. S2BC). CLIP clusters for Rbfox1, 2 and 3 were found adjacent to the majority of alternative exons whose splicing was altered by brain-specific deletion of the Rbfox1 or Rbfox2 genes (Gehman et al., 2011; Gehman et al., 2012). The overlap between Rbfox1, 2, and 3 binding sites supports the hypothesis that functional redundancy reduces the magnitude of splicing changes in Rbfox knockout mice.

The HMW and soluble fractions differed dramatically in the positions of Rbfox binding. In other cells, most unspliced RNA was found in the HMW pellet even after stringent wash conditions (Bhatt et al., 2012; Khodor et al., 2011; Pandya-Jones and Black, 2009). In

agreement with this, the majority of Rbfox binding in the soluble fraction from brain was in 3′ UTR regions. (Fig. 2A), whereas 90% of crosslinking events from the HMW fraction were in introns, indicating predominant Rbfox association with unspliced RNA in this compartment. The patterns of Rbfox binding are illustrated on the *Snap25* transcript (Fig. 2B), which contains a pair of Rbfox-regulated mutually exclusive exons (Gehman et al., 2012; Gehman et al., 2011; Johansson et al., 2008). In the HMW fraction, the majority of crosslinking events were in the intron downstream of the two exons, with the 3′ UTR showing only one prominent Rbfox binding cluster. In the soluble fraction, intron clusters were largely absent (in keeping with the spliced structure of the transcript), whereas the 3′ UTR showed a broadly distributed set of clusters (Fig. 2B). Similar patterns of binding were seen for multiple other transcripts (see supplemental data). The 3′ UTR binding in the soluble nuclear fraction was similar to that seen in the cytoplasm (Lee et al., 2016) and may represent processed mRNA that is not yet exported from the nucleus. RT-PCR measurements indicated that unlike the limited intron crosslinking in the soluble fraction, the lack of binding was not due to reduced amounts of 3′ UTR RNA in the HMW fraction (data not shown). The 3′ UTR of Snap25 mRNA was present in both fractions but not bound by Rbfox until release to the soluble pool. The patterns of crosslinking indicate that more than simple (U)GCAUG recognition determines Rbfox binding to RNA.

The nuclear Rbfox isoforms are subunits of a much larger complex of proteins

IP and mass spectrometry indicated that the Rbfox proteins specifically associated with other proteins in the brain HMW fraction (data not shown), but characterization of these complexes required additional purification. To examine Rbfox interactions in detail, we generated HEK293 cell lines stably expressing N-terminally Flag-tagged Rbfox 1, 2, or 3 (Fig. 3A). Each cell line contained a single flipped-in Rbfox transgene expressing physiological or lower levels of protein compared to brain. The Rbfox proteins exhibited the same enrichment in the HMW nuclear fraction of these cells as in neurons (see below). We immunopurified the Rbfox proteins from this fraction. Elution with Flag peptide yielded a defined set of co-purifying proteins seen on coomassie stained gels at nearly equal stoichometry to the tagged Rbfox protein (Fig. 3A). The pattern of copurifying bands was nearly identical for Rbfox1, 2 and 3. Multidimensional protein identification technology (MuDPIT) and immunoblots identified the major interacting partners (Fig. 3A and Fig. S3A). Two splicing factors, hnRNP M and hnRNP H, (which was previously shown to bind to Rbfox2; (Mauger et al., 2008)) were present at slightly higher stoichiometry to Rbfox. Proteins at near equal amounts to Rbfox included matrin3, NF110/NFAR-2, NF45, and the DEAD-box helicase DDX5/p68. Somewhat lower levels of hnRNP U-like-2 and hnRNP C were also present, as were relatives of the above proteins including MyEF2 (an hnRNP M homolog), hnRNP F, and DDX17/p72 (Fig. 3A and S3A). The same set of proteins was found to associate with Rbfox proteins in mouse brain (Fig. 3B and data not shown). Numerous other RNA binding proteins and splicing factors were absent from the Rbfox purifications, including the major SR proteins, hnRNP A1/B2, A2/B1, R, Q, K, PTBP1 and others (Fig. S3A and data not shown).

Some interactions with Rbfox were specific to particular isoforms. NF110/NFAR-2, the largest product of the ILF3 gene has an extended C-terminus absent from the more abundant

NF90/NFAR-1 isoform (Saunders et al., 2001). Notably NF90/NFAR-1 did not copurify with Rbfox proteins (Fig. S3A), implicating the C-terminal domain of NF110 in this interaction (Reichman and Mathews, 2003). Similarly, hnRNP H1 and H2 copurify with Rbfox more efficiently than the homologous hnRNP F (Fig. 3A, Fig. S3A), whereas for hnRNP M and hnRNP C, family members bound with equal efficiency (Fig. 3A and Fig 3B). The Rbfox interacting proteins were not seen in other immunoprecipitates, such as PTBP1, from brain or HEK293 cells. The strikingly similar stoichiometry of the copurifying proteins, their isoform specificity, and the absence of other RNA binding proteins in the isolate indicated that Rbfox bound with a specific set of interactors and was not copurifying with these proteins via a common interaction with RNA.

Since multiple proteins were isolated in amounts equal to the tagged Rbfox, it appeared that the Rbfox proteins associated with a single complex, rather than making multiple independent interactions. To examine this, we immunoprecipitated Flag-tagged hnRNP M and hnRNP H proteins transiently expressed in HEK293T cells (Fig. S3BC). These overexpressed proteins distributed between the soluble nucleoplasm and the HMW fraction. In the HMW but not the soluble nuclear fraction, both hnRNP M and H copurified with the same set of proteins found with Flag-Rbfox. These proteins were again isolated at similar stoichiometry to each other, although in this case less abundantly than the overexpressed hnRNP M or H (Fig. S3BC). HnRNP M interacted with two additional proteins SRSF14 and hnRNP Q/R. The proteins copurified with hnRNP H or M in the absence of co-expressed Rbfox protein, but when HA-tagged Rbfox3 was transfected this protein was isolated with Flag-hnRNP M (Fig. S3B). These results indicate that the Rbfox proteins in the HMW fraction associate with a defined complex of other proteins that can assemble without Rbfox.

To examine the size of the Rbfox complexes we separated the soluble and HMW nuclear fractions from mouse brain by sedimentation through glycerol density gradients (Fig. 3B). Interestingly, the majority of all three Rbfox proteins in the HMW fraction sedimented as a very large protein complex with an average size of 55S (Fig. 3B; See the anti-Rbfox RRM panel). The abundant proteins copurifying with Flag-Rbfox all showed cosedimenting peaks, including hnRNP M/MyEF2, hnRNP H, hnRNP C, NF110, and NF45 (Fig. 3B). Unlike Rbfox where the majority of the protein was 55S in size, portions of the other proteins sedimented as likely monomers (Fractions 1-2) and smaller complexes (Fractions 4-6). In the soluble nuclear fraction, these proteins also sedimented as free proteins and small complexes at the top of the gradient (data not shown). Numerous other splicing factors, including hnRNP A1, hnRNP K, Nova, PTBP2, the SR proteins and others that did not copurify with Rbfox proteins did not sediment in the 55S fraction, but were found as free proteins or complexes up to about 20S in size (Fig. S1). Notably NF90, containing the same N-terminal double-stranded RNA binding domains as NF110 but lacking its C-terminal domain, failed to cosediment with Rbfox just as it did not copurify with the Flag-Rbfox proteins (Fig. 3B).

We also examined gradients of the HMW fraction from HEK293 cells, probing for Rbfox1 and its interacting proteins hnRNP H and M. Similar to brain, all the Flag-Rbfox1 was found at ~55S, accompanied by peaks of hnRNP H and M (Fig. 4A). Some hnRNP H and M were also present as smaller complexes and apparent monomers (Fig. 4A), and only these smaller

forms were seen in the soluble nuclear fraction (Fig. S3D). The 55S peak of hnRNP H and M was also observed in HEK293 cells not expressing an Rbfox transgene (data not shown). Since these cells express low levels of Rbfox2, it is not clear if Rbfox is responsible for the high S value of the H and M proteins, or if additional complexes assemble from these proteins. The data indicate that nearly the entire nuclear pool of Rbfox proteins is associated with a large nuclease-resistant complex of proteins in both the brain and HEK293 cells.

The total mass of one copy of each protein in the flag eluate is not sufficient to yield a 55S complex, which is expected to be in the megadalton range. To further assess the size and heterogeneity of these protein complexes, we analyzed each fraction across the gradient by native protein gel and immunoblot to identify Flag-Rbfox and hnRNP M containing species. Probing these gels with anti-Flag antibody identified slowly migrating complexes in the fractions containing Rbfox protein (Fig. 4B, top). Interestingly, these complexes increased in size in fractions of successively higher S value. This indicates that the Rbfox complexes are heterogeneous, with an average size of 55S. Probing the gel with anti-hnRNP M antibody labeled the same complexes containing Rbfox, a small species in fraction 2 that is likely monomeric hnRNP M, and a complex lacking Rbfox in gradient fractions 2-6 (Fig. 4B, bottom). This complex may be a precursor to the larger 55S population of complexes containing Rbfox.

Taken together these data indicate that the Rbfox proteins assemble with a large complex of proteins containing hnRNP M, hnRNP H, Matrin3, hnRNP U-like-2, hnRNP C, NF110, NF45, and DDX5/17. We call this complex a Large Assembly of Splicing Regulators (LASR). We next examined how the interaction of Rbfox with LASR might affect splicing.

Rbfox can repress splicing through the binding element for another LASR component hnRNP M

The iCLIP and biochemical analyses together indicate that the intron-bound Rbfox protein is all associated with LASR and thus likely regulates splicing as a part of this assembly. LASR components are also found as free proteins and presumably have functions in addition to their role in LASR. The LASR subunit hnRNP M regulates splicing during the epithelial mesenchymal transition (EMT, Hovhannisyan and Carstens, 2007; Xu et al., 2014). Interestingly, the activity but not the expression of hnRNP M was found to change during EMT, whereas Rbfox2 is upregulated during this transition (Venables et al., 2013; Xu et al., 2014). To test the effect of Rbfox on hnRNP M splicing activity, we created a three exon minigene based on DUP51EK (Amir-Ahmady et al., 2005), where the second exon contains an hnRNP M consensus binding motif, UGGUGGUG, as defined by CLIP analysis (Huelga et al., 2012). We mutated other potential hnRNP M binding sites and all GCAUG motifs, to create DUP-51M1. An equivalent minigene carried a mutation in the hnRNP M site (DUP-51ΔMsite; Fig. 5A). In gel shift assays, purified hnRNP M bound this exon but not the mutant exon, whereas purified Rbfox2 did not bind either the wildtype or mutant exon (Fig. S4ABC). Depletion of hnRNP M by RNAi stimulated splicing of DUP-51M1 exon 2, as did mutation of the M site, confirming that hnRNP M acts as a silencer of the exon (Fig. S4D). We also found that hnRNP M crosslinked to DUP-51M1 pre-mRNA *in vivo* and that this crosslinking is reduced by the M site mutation (Fig. S4E).

DUP51M1 and DUP-51ΔMsite were transfected into HEK293T cells, with and without an Rbfox3 expression plasmid. Coexpression of Rbfox3 strongly inhibited target exon splicing of DUP-51M1, but had minimal effect on DUP-51ΔMsite (Fig. 5B). Thus, Rbfox can alter the splicing of an exon containing an hnRNP M site. The *in vivo* association of Rbfox3 with this transcript was confirmed by crosslinking, anti-Flag IP, and RT-PCR of the pre-mRNA (Fig. 5C). The DUP-51M1 transcript was readily detected in the RNA crosslinked to Rbfox3, and this was strongly reduced by mutation of the M site (Fig. 5C Bottom panel). GAPDH RNA, which crosslinked at moderate levels to the over-expressed Rbfox3 was used to normalize band intensities. The M site mutation did not reduce the level of precursor RNA to cause the reduced Rbfox binding (data not shown). The crosslinking of Rbfox3 indicated close proximity to the reporter premRNA that was dependent on the M site.

To generally assess the effect of Rbfox proteins on hnRNP M activity, we profiled exon inclusion across the transcriptome in a modified HEK cell line where the low level of endogenous Rbfox2 was eliminated by CRISPR/Cas9 deletion of an early exon in the Rbfox2 gene (data not shown). Rbfox1 was introduced at the flip-in locus to yield two cell lines plus and minus Rbfox1 expression (Fig. 6). HnRNP M could be efficiently depleted from both lines by RNAi without affecting Rbfox1 expression (Fig. 6A). Profiling alternative exon use in the four conditions in triplicate by RNAseq and rMATS (Tables S1B and S4; Shen et al., 2014), we identified hnRNP M dependent exons in the presence of Rbfox1, and Rbfox1 dependent exons in the presence hnRNP M (Fig. 6BC). We found that the effect of hnRNP M on both exon activation and exon repression was strikingly reduced when Rbfox1 was absent (Fig. 6B). Of 225 exons whose inclusion was increased or decreased by M depletion in Rbfox1 expressing cells, 144 showed a 15% or greater reduction in this effect in the absence of Rbfox1. To control for bias arising from exon selection, we carried out the reverse analysis of hnRNP M dependent exons defined in the absence Rbfox1. A significantly smaller fraction of these exons were sensitive to Rbfox1 (two-sided p-value $< 2.0x10^{-5}$ by Fisher's exact test). Thus the shift in splicing observed in Fig. 6B was not due to biassed exon selection. These results confirmed that hnRNP M activity was affected by Rbfox.

Reciprocal analyses examined the dependence of exons on Rbfox1 in the presence and absence of hnRNP M (Fig. 6C). RNAi depletion of hnRNP M was not as stringent as Rbfox knockout, leaving about 10% of the endogenous hnRNP M and all of the possibly redundant paralog MyEF2 (data not shown). Nevertheless, of 726 Rbfox1 dependent exons identified in the hnRNP M expressing cells, 329 were less affected by Rbfox1 when hnRNP M was absent (defining the same parameters as 6B). We found that depletion of other LASR components often inhibited cell growth, and/or altered expression of Rbfox proteins. Testing the effects of these proteins on Rbfox activity will likely require different approaches.

The binding of Rbfox to its target element is affected by adjacent sequence motifs

To assess whether LASR components affect where Rbfox binds, we analyzed sites of Rbfox crosslinking for enriched binding motifs. Among the LASR subunits, hnRNP M binds to GU-rich motifs (Huelga et al., 2012), hnRNP C to polyU sequences (Gorlach et al., 1994; König et al., 2010; Swanson and Dreyfuss, 1988), and hnRNP H to polyG and GGGA

sequences (Caputi and Zahler, 2001; Chou et al., 1999; Huelga et al., 2012). We defined high confidence binding sites as intronic sequences containing overlapping iCLIP clusters for all three Rbfox proteins in either the forebrain or hindbrain HMW fractions. These regions were analyzed for pentamer frequencies (See Supplemental Experimental Procedures; Table S2). Based on the previous CLIP analyses (Huelga et al., 2012), we defined possible hnRNP M binding motifs as all pentamers containing 3 G's and 2 U's or 3 U's and 2 G's but without more than 2 Gs or Us in a row. This definition includes all the described binding pentamers, but it is likely that some sequences within this group bind hnRNP M better than others. HnRNP C pentamers included U5 and all pentamers containing 4 continuous U nucleotides. Similarly, hnRNP H pentamers included G5 and all pentamers containing 4 continuous G's. Within the large set of Rbfox binding regions, both hnRNP M and hnRNP C motifs were highly enriched, whereas hnRNP H motifs were depleted relative to a control distribution (Fig. S5).

GCAUG was the most enriched pentamer in the high confidence binding regions and this motif was often aligned precisely at the crosslink site (Fig. 2B and S5). However, as seen previously, many iCLIP clusters did not contain the GCAUG motif (Jangi et al., 2014; Lovci et al., 2013; Weyn-Vanhentenryck et al., 2014; Yeo et al., 2009). We subdivided the intronic binding regions into two sets: A) those containing a GCAUG or a UGCAU within ± 40 nucleotides of the crosslink site and B) those without such a proximal Rbfox binding motif. These two sets of sequences were analyzed for pentamer frequencies (Fig. 7A and 7B, with all motif scores in Table S3). Binding regions in Set A showed the expected enrichment of its component GCAUG and UGCAU pentamers (Fig. S5). In the Set B binding regions, U pentamers were the most enriched motifs, and were more common than in Set A (compare Fig. 7A and 7B). Similar to the entire high confidence set of iCLIP clusters (Fig. S5), GU pentamers were highly enriched in both subsets of binding regions. These data indicate that binding sites for other LASR components are commonly found adjacent to sites of Rbfox binding.

To examine the positions of particular motifs relative to the crosslink sites, we further refined two smaller groups of intronic Rbfox iCLIP clusters. Group 1 contained a GCAUG within five nucleotides upstream or downstream of the crosslinking site defined as position 0 (orange lines in Fig 7C). As seen previously (Jangi et al., 2014; Weyn-Vanhentenryck et al., 2014), the GCAUG pentamer most frequently began at either position −4 or 0, consistent with crosslinking to the second or the first guanine of a GCAUG motif (Fig. 7C, top). The second group of clusters (red lines in Fig. 7C) contained crosslink sites more than 100 nt away from the nearest GCAUG. In Group 2 clusters, Rbfox crosslinking is presumably determined by other interactions than GCAUG recognition, although it is possible that secondary structure brings a distal GCAUG motif close to the crosslinked region. The U5 motif was strongly enriched precisely at the crosslink sites of the Group 2 clusters (red line, Fig. 7C bottom), with the most frequent crosslink at U2. This motif showed no enrichment at particular positions adjacent to the GCAUG crosslink sites (orange line).

Individual GU pentamers were enriched at particular positions in both groups of crosslinking sites (Fig. 7C shows the GU pentamers with the top z-scores). In Group 1 clusters, these GU pentamers were enriched at upstream and downstream positions directly abutting the

crosslinked GCAUG, as well as further upstream of the GCAUG motif. Since all the Rbfox is assembled with LASR, the common position of these pentamers presumably reflects the binding of another LASR protein – most likely hnRNP M. The Group 2 clusters showed different patterns of GU pentamer placement (Fig. 7C, red lines), with peaks very close to the crosslink site, and dispersed enrichment in the adjacent sequence.

The most enriched GU-rich pentamer in these Group 2 clusters was UGUUG. To examine the activity of this element in splicing, we made a new splicing reporter with the duplicated element UGUUGUGUUG in the exon (DUP-50M1, diagramed in Fig. S6A). This fused element also contains a UGUGU pentamer that is enriched in Group 2 clusters. Purified hnRNP M but not Rbfox2 bound this exon *in vitro*, and the M binding was eliminated by mutation of the element (Fig. S4ABC). This element but not its mutant rendered the exon repressible by Rbfox3 and stimulated crosslinking of Rbfox3 to the transcript *in vivo* (Fig. S6BC), similar to the hnRNP M element defined by iCLIP (Fig. 5BC).

For every GCAUG sequence within an iCLIP cluster, there can be dozens of exact UGCAUG sequences within the same transcript that do not exhibit crosslinking and presumably do not bind Rbfox. To examine the contribution of adjacent nucleotides to Rbfox binding, we aligned the central GCAUG motifs from the Group 1 clusters and plotted the nucleotide frequency at adjacent positions. The highest probability sequence flanking the GCAUG from position −15 to position +15 consisted of alternating G and U nucleotides (Fig. 7D, top). This pattern was compared to UGCAUG hexamers from introns containing iCLIP clusters, but which did not generate a cluster themselves. Nucleotides adjacent to these non-Rbfox binding hexamers exhibited a different pattern of A and U enrichment (Fig. 7D, middle). GCAUG motifs bound by Rbfox were also more conserved than the unbound motifs, with PhyloP conservation scores peaking within the GCAUG and extending into adjacent nucleotides (Fig. 7D, bottom). These data indicate that the surrounding nucleotide context of a (U)GCAUG element contributes to its recruitment of an Rbfox protein.

Discussion

A Large Protein Assembly for Rbfox Proteins

Much of splicing occurs in conjunction with transcription, and splicing factors are concentrated adjacent to active loci in nuclear speckles thought to consist of dense networks of intermolecular interactions. After nuclear lysis, unspliced RNA remains associated with chromatin and other high molecular weight assemblies. However, biochemical analyses of pre-mRNA splicing usually employ proteins and RNPs eluted from intact nuclei at moderate salt that may not engage in all interactions defining their function. To assess the contacts of splicing regulators in compartments more immobile than the soluble nucleoplasm, we lysed nuclei under mild conditions and examined how proteins partition between the pellet and the supernatant upon centrifugation. The Rbfox proteins were largely found in the HMW pellet, containing chromatin, nuclear speckle components, and unspliced RNA. Splicing regulators were associated with RNA in this fraction, and extraction of the pellet with Benzonase released them in soluble form. In this preparation the Rbfox proteins were associated with a multimeric complex, the Large Assembly of Splicing Regulators, LASR. It will be

interesting to examine other regulators in these fractions and perhaps find other new interactions.

The Rbfox protein in the HMW extract was entirely associated with LASR. Isolation of LASR via a tagged Rbfox protein or tagged hnRNP M or H yielded approximately equal quantities of hnRNP M, hnRNP H, and tagged Rbfox, and only slightly lower amounts of Matrin3, hnRNP U-like2, hnRNP C, NF110, NF45, and DDX5. The near equimolar stoichiometry of the components when isolated with different tagged subunits indicated that LASR assembled via specific protein-protein interactions and was not a random aggregation of proteins released by the nuclease. Similarly, the absence of other RNA binding proteins in the complex, and its resistance to extensive nuclease treatment, indicated that the LASR subunits were not held together by binding to a common RNA. This nuclease resistance distinguishes LASR from previously characterized RNP assemblies such as the 40S hnRNP particle, the DBIRD complex, and the higher-order exon junction complex (Close et al., 2012; Singh et al., 2012; Walker et al., 1980).

LASR subunits were present as free proteins, small complexes that contain components other than Rbfox, and large 55S assemblies that contain Rbfox. The 55S complexes were heterogeneous in size yet still yielded equivalent stoichiometries of all the components, indicating that they may be higher order assemblies of a unit complex. The unit LASR complex is present in cells without Rbfox (Fig. 4B, Fig. S3C). This may multimerize to create the 55S forms, or interact with a much larger but substoichometric structure to yield its high S value. Given that all of the Rbfox is in this larger form, it is possible that Rbfox itself mediates the multimerization. In the brain, nuclear Rbfox1 and Rbfox3 were almost entirely associated with the 55S complex. Rbfox2 bound this complex, but was also in light fractions, indicating a possible functional difference of Rbfox2. It will be interesting to identify interactions that hold the LASR subunits together, that allow recruitment of Rbfox, and that mediate its higher order assembly.

The components of LASR engage in a variety of other interactions. LASR shares several components with one of two described microprocessor complexes, including NF45, DDX5, DDX17, hnRNP M, and hnRNP H (Gregory et al., 2004). Instead of Rbfox the microprocessor contains Drosha and DGCR8 that carry out miRNA processing. Other described Rbfox interactions include with U1C, hnRNP K, Sam68, RALY, PSF, TFG, and Ataxin2, as well as the aforementioned hnRNP H contact (Huang et al., 2012; Kim et al., 2011; Mauger et al., 2008; Shibata et al., 2000; Sun et al., 2012). Recombinant Rbfox added to an *in vitro* splicing extract inhibited assembly of a pre-spliceosomal E-complex on an Rbfox-repressed exon (Fukumura et al., 2007; Zhou and Lou, 2008). This activity will be interesting to assess for involvement of the LASR complex.

Rbfox Regulation of Splicing in the Context of LASR

We find that the expression of Rbfox altered the activity of hnRNP M in controlling splicing, and that M binding sites increased the crosslinking of Rbfox to a reporter RNA *in vivo*. Thus, the hnRNP M component of LASR can apparently allow Rbfox to alter splicing through an indirect interaction with the RNA. In examining what constitutes a functional binding site, we found that sequences adjacent to Rbfox-crosslinked GCAUG pentamers

were enriched for motifs that potentially bind hnRNP M. We further found that atypical non-(U)GCAUG sites of Rbfox crosslinking were enriched for M and C motifs, possibly indicative of LASR mediated recruitment of Rbfox. Although additional work is needed to confirm this mechanism, such an hnRNP M/Rbfox interaction can explain how the activity but not the expression of hnRNP M increases during the EMT (Venables et al., 2013; Xu et al., 2014).

The multiple RNA binding domains within LASR raise questions regarding the optimal arrangement of regulatory motifs and how the architecture of the complex might enforce co-recognition of certain motifs. The enrichment of GU-rich motifs adjacent to GCAUG binding elements may derive from the hnRNP M in the LASR contacting the RNA simultaneously with Rbfox. However, other GU binding proteins cannot be ruled out. In *C. elegans*, an Rbfox family member can cooperatively assemble with the Sup12 protein binding to an adjacent GU-rich motif (Kuwasako et al., 2014). It is not clear whether mammalian Sup12-like proteins also cooperate with Rbfox or bind LASR. Substantial efforts are being directed at understanding a “splicing code” that would predict the splicing pattern of a pre-mRNA from its sequence (Barash et al., 2010; Zhang et al., 2010). A group of splicing regulators acting within a common complex provides a mechanistic explanation for the co-occurrence of certain binding motifs.

The non-RRM domain proteins of LASR also have interesting features. The double-stranded RNA binding protein NF110/NFAR2 and the helicase DDX5 were shown to interact and to affect transcriptional regulation (Fuller-Pace, 2013; Ogilvie et al., 2003; Reichman and Mathews, 2003; Saunders et al., 2001). DEAD-box proteins like DDX5 often have lower RNA helicase activity than the DEAH-box family and may instead act as switches to control assembly steps, with ATP hydrolysis toggling the protein between conformational or binding states (Singh et al., 2015). Studies demonstrate DDX5 involvement in splicing of particular exons where it may alter assembly of pre-mRNP complexes (Guil et al., 2003; Kar et al., 2011; Liu, 2002).

Most attention has focused on the RNA recognition properties of splicing regulators, but these proteins also engage in complex protein/protein interactions. An Rbfox splice variant lacking most of the RNA binding domain, but retaining the N and C terminal domains can block splicing activation but not splicing repression by full-length Rbfox (Damianov and Black, 2010). The C-terminal domain is required for both splicing repression and activation by an MS2-tethered Rbfox protein (Sun et al., 2012). The significance of the Rbfox1 and Rbfox3 C-terminal domains is underscored by their mutation in familial epileptic syndromes (Lal et al., 2013a; Lal et al., 2013b). Elucidating the consequences of these mutations, as well as understanding Rbfox1 roles in autism spectrum disorders and spinal cerebellar ataxia, will require a clearer description of Rbfox interactions in nuclear and cytoplasmic mRNA metabolism.

Experimental Procedures

Cell culture and tissue isolation

Stable HEK293 lines expressing HA-Flag-tagged Rbfox1, 2, or 3 proteins were prepared using the Flp-In™ T-REx™ System (Life Technologies). An Rbfox2 deficient clone derived from this cell line was obtained by CRISPR/Cas9-guided deletions in the first constitutive Rbfox2 exon. Brain tissue was obtained from 6 week old C57BL/6J male mice (Charles River). Transfection of HEK293 cells was as described (Damianov and Black, 2010). For transient expression of recombinant proteins cells were harvested 48 hours post-transfection or post-induction with 0.5 μg /ml doxycycline. For RNAi, hnRNP M was targeted with shRNAs as described in the Supplemental Experimental Procedures.

RT-PCR

Total RNA was extracted with TRIzol® (LifeTech) from cells or tissues. DNA was removed with RQ1 DNase. Reverse transcription was carried with SuperScript® III (Life Tech) and gene-specific reverse primers. Minigene and GAPDH products were amplified for 15-18 PCR cycles and detected as described (Damianov and Black, 2010). Primer and minigene sequences are listed in Extended Experimental Procedures.

RNA-protein crosslinking *in vivo*

Monolayer HEK293T cultures were irradiated with UV (254 nm) at 75 mJ/cm^2 on ice in a Stratalinker 1800 (Stratagene). Mouse brain samples were triturated in ice-cold HBSS solution and UV-irradiated at 600 mJ/cm^2.

Preparation of whole cell lysates for reporter experiments

UV-irradiated HEK293T cells were lysed 5 min on ice with 10 packed cell volumes of buffer (20 mM HEPES-KOH pH 7.5, 150 mM NaCl, 0.5 mM DTT, 1 mM EDTA, 0.6% Triton X-100, 0.1% SDS, and 50 μg /μl yeast tRNA) and centrifuged at 20,000x g for 5 min at 4 °C. The supernatants were 5x diluted with buffer (20 mM HEPES-KOH pH 7.5, 150 mM NaCl, 0.5 mM DTT, 1 mM EDTA, 1.25x cOmplete protease inhibitors (Roche), and 50 μg/ul yeast tRNA). Lysates were spun for 10 min at 20,000x g, 4 °C prior to IP.

Subcellular fractionation

Nuclei from cell cultures or tissues were purified as described (Grabowski, 2005), resuspended in 10 volumes of buffer (10 mM HEPES-KOH pH 7.6, 15 mM KCl, 1 mM EDTA, 0.15 mM Spermine, 0.5 mM Spermidine), and pelleted at 1,000x g for 5 min at 4 °C. Nuclei were lysed for 5 minutes in 10 volumes of ice-cold lysis buffer (20 mM HEPES-KOH pH 7.5, 150 mM NaCl, 1.5 mM MgCl2, 0.5 mM DTT, 1.25x protease inhibitors, and 0.6% Triton X-100). Soluble and HMW fractions were separated by centrifugation at 20,000x g for 5 min at 4 °C. Samples for iCLIP are described in the supplementary material. To extract nuclease-resistant protein complexes, the soluble fraction was removed and an equal volume of lysis buffer added to the HMW pellet. Soluble and HMW fractions were incubated at 25 °C on a rotator with 5 U/μl of Benzonase® (Sigma) until the HMW pellet was resuspended, and then cleared by centrifugation for 10 min at 20,000x g, 4 °C.

Immunoprecipitation

Nuclear fractions or whole cell lysates were incubated overnight at 4 °C with 5-7.5 µl packed M2 FLAG agarose beads (Sigma). For nuclear fractions beads were washed four times with wash buffer (20 mM HEPES-KOH pH 7.5, 150 mM NaCl, and 0.05% Triton-X100). For whole cell lysates beads were washed five times with wash buffer containing 1M NaCl, and twice with standard wash buffer. Flag-tagged proteins were eluted from beads over two hours at 4 °C in 50-100 µl of Elution buffer (20 mM HEPES-KOH pH 7.5, 100 mM NaCl, and 150 ng/µl of 3xFLAG peptide (Sigma)). RNA-protein crosslinks were eluted with Elution buffer plus 5 µg of yeast tRNA.

Protein analysis

Immunoprecipitated proteins were subjected to Multidimensional Protein Identification (MuDPIT) as described (Sharma et al., 2014), and analyzed by SDS-PAGE with immunoblotting, or protein staining as described (Damianov and Black, 2010). Protein complexes were resolved on 10-50% glycerol gradients (20 mM HEPES-KOH pH 7.5, 150 mM NaCl, 0.5 mM DTT, and 1x Protease Inhibitor) in 14x89 mm tubes (Beckman Coulter). Extracts (250 µl) were loaded and spun in a SW41Ti rotor (Beckman Coulter) at 32,000x RPM for 12 hours at 4 °C. Gradients were fractionated top to bottom into 24x500ul fractions. Fractions were analyzed by immunoblot, or resolved on 3-12% NativePAGE™ Novex® Bis-Tris Gels (Life Tech.). Primary antibodies are listed in Extended Experimental Procedures.

Individual-nucleotide resolution UV cross-linking and immunoprecipitation (iCLIP)

iCLIP libraries were prepared following (König et al., 2010), with changes to allow for the differing RNA content of the cellular fractions. iCLIP libraries were sequenced on a HiSeq2000 (Illumina). Data analyses were performed as in (König et al., 2010) with few modifications. In brief, PCR duplicate iCLIP reads were removed using random barcodes. Unique reads were mapped to mouse genome mm9/NCBI37 using Bowtie allowing two mismatches (Langmead et al., 2009). Mapped reads were assigned to the longest transcripts in the Known Gene table (Hsu et al., 2006) and divided into 5′ UTR, CDS, intron, and 3′ UTR regions. Motif enrichment and the modified iCLIP protocol are described in the Extended Experimental Procedures.

Genome-wide splicing analysis

Total TRIzol® extracted RNA was treated with TURBO DNase (Ambion), and polyA plus RNA isolated on Oligo-dT. cDNA libraries were prepared using TruSeq Kits (Illumina). Read properties are shown in Table S1B. Alternative splicing was analyzed by rMATS (Shen et al., 2014) and expressed as changes in percent-spliced-in values (ΔPSI). Exons showing splicing change ($|\Delta PSI|>10$ with FDR less than 0.5) between control and hnRNP M-depleted samples from Flag-Rbfox1-expressing cells were considered hnRNP M regulatory targets. Similarly, Rbfox1-dependent exons were defined in cells expressing hnRNP M.

Public Data Submission

The iCLIP and RNAseq data is available at NCBI GEO under the accession number GSE71468: (http://www.ncbi.nlm.nih.gov/geo/query/acc.cgi?token=mfahuaimrbmtdyv&acc=GSE71468).

Supplementary Material

Refer to Web version on PubMed Central for supplementary material.

Acknowledgements

We thank Julian König and Jernej Ule for communicating the iCLIP protocol ahead of publication, and Celine Vuong and Anthony Linares for critical reading of the manuscript. This work was supported by the Howard Hughes Medical Institute (DLB), NIH grants R21 MH101684 (KCM), R01 GM088432 (YX), R01 GM105431 (YX), and R01 GM089778 (JAW), a NARSAD Young Investigator Award (JAL), the China Scholarship Council (YY), an Alfred P Sloan Fellowship (YX), and the Broad Center for Stem Cell Research at UCLA.

References

Amir-Ahmady B, Boutz PL, Markovtsov V, Phillips ML, Black DL. Exon repression by polypyrimidine tract binding protein. RNA. 2005; 11:699–716. [PubMed: 15840818]

Auweter SD, Fasan R, Reymond L, Underwood JG, Black DL, Pitsch S, Allain FH. Molecular basis of RNA recognition by the human alternative splicing factor Fox-1. EMBO J. 2006; 25:163–173. [PubMed: 16362037]

Barash Y, Calarco JA, Gao W, Pan Q, Wang X, Shai O, Blencowe BJ, Frey BJ. Deciphering the splicing code. Nature. 2010; 465:53–59. [PubMed: 20445623]

Bhalla K, Phillips HA, Crawford J, McKenzie OL, Mulley JC, Eyre H, Gardner AE, Kremmidiotis G, Callen DF. The de novo chromosome 16 translocations of two patients with abnormal phenotypes (mental retardation and epilepsy) disrupt the A2BP1 gene. J. Hum. Genet. 2004; 49:308–311. [PubMed: 15148587]

Bhatt DM, Pandya-Jones A, Tong AJ, Barozzi I, Lissner MM, Natoli G, Black DL, Smale ST. Transcript dynamics of proinflammatory genes revealed by sequence analysis of subcellular RNA fractions. Cell. 2012; 150:279–290. [PubMed: 22817891]

Bill BR, Lowe JK, Dybuncio CT, Fogel BL. Orchestration of neurodevelopmental programs by RBFOX1: implications for autism spectrum disorder. Int. Rev. Neurobiol. 2013; 113:251–267. [PubMed: 24290388]

Braeutigam C, Rago L, Rolke A, Waldmeier L, Christofori G, Winter J. The RNA-binding protein Rbfox2: an essential regulator of EMT-driven alternative splicing and a mediator of cellular invasion. Oncogene. 2014; 33:1082–1092. [PubMed: 23435423]

Caputi M, Zahler AM. Determination of the RNA binding specificity of the heterogeneous nuclear ribonucleoprotein (hnRNP) H/H'/F/2H9 family. The J. Biol. Chem. 2001; 276:43850–43859. [PubMed: 11571276]

Chou MY, Rooke N, Turck CW, Black DL. hnRNP H is a component of a splicing enhancer complex that activates a c-src alternative exon in neuronal cells. Mol. Cell. Biol. 1999; 19:69–77. [PubMed: 9858532]

Close P, East P, Dirac-Svejstrup AB, Hartmann H, Heron M, Maslen S, Chariot A, Soding J, Skehel M, Svejstrup JQ. DBIRD complex integrates alternative mRNA splicing with RNA polymerase II transcript elongation. Nature. 2012; 484:386–389. [PubMed: 22446626]

Crooks GE, Hon G, Chandonia JM, Brenner SE. WebLogo: a sequence logo generator. Genome res. 2004; 14:1188–1190. [PubMed: 15173120]

Damianov A, Black DL. Autoregulation of Fox protein expression to produce dominant negative splicing factors. RNA. 2010; 16:405–416. [PubMed: 20042473]

Fu XD, Ares M Jr. Context-dependent control of alternative splicing by RNA-binding proteins. Nat. Rev. Genet. 2014; 15:689–701. [PubMed: 25112293]

Fukumura K, Kato A, Jin Y, Ideue T, Hirose T, Kataoka N, Fujiwara T, Sakamoto H, Inoue K. Tissue-specific splicing regulator Fox-1 induces exon skipping by interfering E complex formation on the downstream intron of human F1gamma gene. Nucleic Acids Res. 2007; 35:5303–5311. [PubMed: 17686786]

Fuller-Pace FV. The DEAD box proteins DDX5 (p68) and DDX17 (p72): multi-tasking transcriptional regulators. Biochim. Biophys. Acta. 2013; 1829:756–763. [PubMed: 23523990]

Gehman LT, Meera P, Stoilov P, Shiue L, O'Brien JE, Meisler MH, Ares M Jr. Otis TS, Black DL. The splicing regulator Rbfox2 is required for both cerebellar development and mature motor function. Genes Dev. 2012; 26:445–460. [PubMed: 22357600]

Gehman LT, Stoilov P, Maguire J, Damianov A, Lin CH, Shiue L, Ares M Jr. Mody I, Black DL. The splicing regulator Rbfox1 (A2BP1) controls neuronal excitation in the mammalian brain. Nat. Genet. 2011; 43:706–711. [PubMed: 21623373]

Gorlach M, Burd CG, Dreyfuss G. The determinants of RNA-binding specificity of the heterogeneous nuclear ribonucleoprotein C proteins. J. Biol. Chem. 1994; 269:23074–23078. [PubMed: 8083209]

Grabowski PJ. Splicing-active nuclear extracts from rat brain. Methods. 2005; 37:323–330. [PubMed: 16314261]

Gregory RI, Yan KP, Amuthan G, Chendrimada T, Doratotaj B, Cooch N, Shiekhattar R. The Microprocessor complex mediates the genesis of microRNAs. Nature. 2004; 432:235–240. [PubMed: 15531877]

Guil S, Gattoni R, Carrascal M, Abian J, Stevenin J, Bach-Elias M. Roles of hnRNP A1, SR proteins, and p68 helicase in c-H-ras alternative splicing regulation. Mol. Cell. Biol. 2003; 23:2927–2941. [PubMed: 12665590]

Hovhannisyan RH, Carstens RP. Heterogeneous ribonucleoprotein m is a splicing regulatory protein that can enhance or silence splicing of alternatively spliced exons. J. Biol. Chem. 2007; 282:36265–36274. [PubMed: 17959601]

Hsu F, Kent WJ, Clawson H, Kuhn RM, Diekhans M, Haussler D. The UCSC Known Genes. Bioinformatics. 2006; 22:1036–1046. [PubMed: 16500937]

Huang SC, Ou AC, Park J, Yu F, Yu B, Lee A, Yang G, Zhou A, Benz EJ Jr. RBFOX2 promotes protein 4. 1R exon 16 selection via U1 snRNP recruitment. Mol. Cell. Biol. 2012; 32:513–526. [PubMed: 22083953]

Huelga SC, Vu AQ, Arnold JD, Liang TY, Liu PP, Yan BY, Donohue JP, Shiue L, Hoon S, Brenner S, et al. Integrative genome-wide analysis reveals cooperative regulation of alternative splicing by hnRNP proteins. Cell Rep. 2012; 1:167–178. [PubMed: 22574288]

Jangi M, Boutz PL, Paul P, Sharp PA. Rbfox2 controls autoregulation in RNA-binding protein networks. Genes Dev. 2014; 28:637–651. [PubMed: 24637117]

Jin Y, Suzuki H, Maegawa S, Endo H, Sugano S, Hashimoto K, Yasuda K, Inoue K. A vertebrate RNA-binding protein Fox-1 regulates tissue-specific splicing via the pentanucleotide GCAUG. EMBO J. 2003; 22:905–912. [PubMed: 12574126]

Johansson JU, Ericsson J, Janson J, Beraki S, Stanic D, Mandic SA, Wikstrom MA, Hokfelt T, Ogren SO, Rozell B, et al. An ancient duplication of exon 5 in the Snap25 gene is required for complex neuronal development/function. PLoS Genet. 2008; 4:e1000278. [PubMed: 19043548]

Kar A, Fushimi K, Zhou X, Ray P, Shi C, Chen X, Liu Z, Chen S, Wu JY. RNA helicase p68 (DDX5) regulates tau exon 10 splicing by modulating a stem-loop structure at the 5′ splice site. Mol. Cell. Biol. 2011; 31:1812–1821. [PubMed: 21343338]

Khodor YL, Rodriguez J, Abruzzi KC, Tang CH, Marr MT 2nd, Rosbash M. Nascent-seq indicates widespread cotranscriptional pre-mRNA splicing in Drosophila. Genes Dev. 2011; 25:2502–2512. [PubMed: 22156210]

Kim KK, Kim YC, Adelstein RS, Kawamoto S. Fox-3 and PSF interact to activate neural cell-specific alternative splicing. Nucleic Acids Res. 2011; 39:3064–3078. [PubMed: 21177649]

König J, Zarnack K, Rot G, Curk T, Kayikci M, Zupan B, Turner DJ, Luscombe NM, Ule J. iCLIP reveals the function of hnRNP particles in splicing at individual nucleotide resolution. Nat. Struct. Mol. Biol. 2010; 17:909–915. [PubMed: 20601959]

Kuroyanagi H. Fox-1 family of RNA-binding proteins. Cell. Mol. Life Sci. 2009; 66:3895–3907. [PubMed: 19688295]

Kuwasako K, Takahashi M, Unzai S, Tsuda K, Yoshikawa S, He F, Kobayashi N, Guntert P, Shirouzu M, Ito T, et al. RBFOX and SUP-12 sandwich a G base to cooperatively regulate tissue-specific splicing. Nat. Struct. Mol. Biol. 2014; 21:778–786. [PubMed: 25132178]

Lal D, Reinthaler EM, Altmuller J, Toliat MR, Thiele H, Nurnberg P, Lerche H, Hahn A, Moller RS, Muhle H, et al. RBFOX1 and RBFOX3 mutations in rolandic epilepsy. PloS ONE. 2013a; 8:e73323. [PubMed: 24039908]

Lal D, Trucks H, Moller RS, Hjalgrim H, Koeleman BP, de Kovel CG, Visscher F, Weber YG, Lerche H, Becker F, et al. Rare exonic deletions of the RBFOX1 gene increase risk of idiopathic generalized epilepsy. Epilepsia. 2013b; 54:265–271. [PubMed: 23350840]

Lambert N, Robertson A, Jangi M, McGeary S, Sharp PA, Burge CB. RNA Bind-n-Seq: Quantitative Assessment of the Sequence and Structural Binding Specificity of RNA Binding Proteins. Mol. Cell. 2014; 54:887–900. [PubMed: 24837674]

Langmead B, Trapnell C, Pop M, Salzberg SL. Ultrafast and memory-efficient alignment of short DNA sequences to the human genome. Genome Biol. 2009; 10:R25. [PubMed: 19261174]

Lee JA, Damianov A, Lin CH, Fontes M, Parikshak NN, Anderson ES, Geschwind DH, Black DL, Martin KC. Cytoplasmic Rbfox1 Regulates the Expression of Synaptic and Autism-Related Genes. Neuron. 2016; 89:113–128. [PubMed: 26687839]

Lee JA, Tang ZZ, Black DL. An inducible change in Fox-1/A2BP1 splicing modulates the alternative splicing of downstream neuronal target exons. Genes Dev. 2009; 23:2284–2293. [PubMed: 19762510]

Lee Y, Rio DC. Mechanisms and Regulation of Alternative Pre-mRNA Splicing. Ann. Rev. Biochem. 2015; 84:291–323. [PubMed: 25784052]

Liu ZR. p68 RNA helicase is an essential human splicing factor that acts at the U1 snRNA-5′ splice site duplex. Mol. Cell. Biol. 2002; 22:5443–5450. [PubMed: 12101238]

Lovci MT, Ghanem D, Marr H, Arnold J, Gee S, Parra M, Liang TY, Stark TJ, Gehman LT, Hoon S, et al. Rbfox proteins regulate alternative mRNA splicing through evolutionarily conserved RNA bridges. Nat. Struct. Mol. Biol. 2013; 20:1434–1442. [PubMed: 24213538]

Mauger DM, Lin C, Garcia-Blanco MA. hnRNP H and hnRNP F complex with Fox2 to silence fibroblast growth factor receptor 2 exon IIIc. Mol. Cell. Biol. 2008; 28:5403–5419. [PubMed: 18573884]

Misteli T, Caceres JF, Clement JQ, Krainer AR, Wilkinson MF, Spector DL. Serine phosphorylation of SR proteins is required for their recruitment to sites of transcription in vivo. J. Cell Biol. 1998; 143:297–307. [PubMed: 9786943]

Nakahata S, Kawamoto S. Tissue-dependent isoforms of mammalian Fox-1 homologs are associated with tissue-specific splicing activities. Nucleic Acids Res. 2005; 33:2078–2089. [PubMed: 15824060]

Ogilvie VC, Wilson BJ, Nicol SM, Morrice NA, Saunders LR, Barber GN, Fuller-Pace FV. The highly related DEAD box RNA helicases p68 and p72 exist as heterodimers in cells. Nucleic Acids Res. 2003; 31:1470–1480. [PubMed: 12595555]

Pandya-Jones A, Black DL. Co-transcriptional splicing of constitutive and alternative exons. RNA. 2009; 15:1896–1908. [PubMed: 19656867]

Reichman TW, Mathews MB. RNA binding and intramolecular interactions modulate the regulation of gene expression by nuclear factor 110. RNA. 2003; 9:543–554. [PubMed: 12702813]

Saunders LR, Perkins DJ, Balachandran S, Michaels R, Ford R, Mayeda A, Barber GN. Characterization of two evolutionarily conserved, alternatively spliced nuclear phosphoproteins, NFAR-1 and -2, that function in mRNA processing and interact with the double-stranded RNA-dependent protein kinase, PKR. J. Biol. Chem. 2001; 276:32300–32312. [PubMed: 11438536]

Sharma S, Wongpalee SP, Vashisht A, Wohlschlegel JA, Black DL. Stem-loop 4 of U1 snRNA is essential for splicing and interacts with the U2 snRNP-specific SF3A1 protein during spliceosome assembly. Genes Dev. 2014; 28:2518–2531. [PubMed: 25403181]

Shen S, Park JW, Lu ZX, Lin L, Henry MD, Wu YN, Zhou Q, Xing Y. rMATS: robust and flexible detection of differential alternative splicing from replicate RNA-Seq data. Proc. Natl. Acad. Sci. USA. 2014; 111:E5593–5601. [PubMed: 25480548]

Shibata H, Huynh DP, Pulst SM. A novel protein with RNA-binding motifs interacts with ataxin-2. Hum. Mol. Genet. 2000; 9:1303–1313. [PubMed: 10814712]

Singh G, Kucukural A, Cenik C, Leszyk JD, Shaffer SA, Weng Z, Moore MJ. The cellular EJC interactome reveals higher-order mRNP structure and an EJC-SR protein nexus. Cell. 2012; 151:750–764. [PubMed: 23084401]

Singh G, Pratt G, Yeo GW, Moore MJ. The Clothes Make the mRNA: Past and Present Trends in mRNP Fashion. Ann. Rev. Biochem. 2015; 84:325–354. [PubMed: 25784054]

Sun S, Zhang Z, Fregoso O, Krainer AR. Mechanisms of activation and repression by the alternative splicing factors RBFOX1/2. RNA. 2012; 18:274–283. [PubMed: 22184459]

Swanson MS, Dreyfuss G. Classification and purification of proteins of heterogeneous nuclear ribonucleoprotein particles by RNA-binding specificities. Mol. Cell. Biol. 1988; 8:2237–2241. [PubMed: 3386636]

Tang ZZ, Zheng S, Nikolic J, Black DL. Developmental control of CaV1.2 L-type calcium channel splicing by Fox proteins. Mol. Cell. Biol. 2009; 29:4757–4765. [PubMed: 19564422]

Tripathi V, Song DY, Zong X, Shevtsov SP, Hearn S, Fu XD, Dundr M, Prasanth KV. SRSF1 regulates the assembly of pre-mRNA processing factors in nuclear speckles. Mol. Biol. Cell. 2012; 23:3694–3706. [PubMed: 22855529]

Venables JP, Brosseau JP, Gadea G, Klinck R, Prinos P, Beaulieu JF, Lapointe E, Durand M, Thibault P, Tremblay K, et al. RBFOX2 is an important regulator of mesenchymal tissue-specific splicing in both normal and cancer tissues. Mol. Cell. Biol. 2013; 33:396–405. [PubMed: 23149937]

Walker BW, Lothstein L, Baker CL, LeStourgeon WM. The release of 40S hnRNP particles by brief digestion of HeLa nuclei with micrococcal nuclease. Nucleic Acids Res. 1980; 8:3639–3657. [PubMed: 7433102]

Weyn-Vanhentenryck SM, Mele A, Yan Q, Sun S, Farny N, Zhang Z, Xue C, Herre M, Silver PA, Zhang MQ, et al. HITS-CLIP and integrative modeling define the Rbfox splicing-regulatory network linked to brain development and autism. Cell Rep. 2014; 6:1139–1152. [PubMed: 24613350]

Wuarin J, Schibler U. Physical isolation of nascent RNA chains transcribed by RNA polymerase II: evidence for cotranscriptional splicing. Mol. Cell. Biol. 1994; 14:7219–7225. [PubMed: 7523861]

Xu Y, Gao XD, Lee JH, Huang H, Tan H, Ahn J, Reinke LM, Peter ME, Feng Y, Gius D, et al. Cell type-restricted activity of hnRNPM promotes breast cancer metastasis via regulating alternative splicing. Genes Dev. 2014; 28:1191–1203. [PubMed: 24840202]

Yeo GW, Coufal NG, Liang TY, Peng GE, Fu XD, Gage FH. An RNA code for the FOX2 splicing regulator revealed by mapping RNA-protein interactions in stem cells. Nat. Struct. Mol. Biol. 2009; 16:130–137. [PubMed: 19136955]

Zhang C, Frias MA, Mele A, Ruggiu M, Eom T, Marney CB, Wang H, Licatalosi DD, Fak JJ, Darnell RB. Integrative modeling defines the Nova splicing-regulatory network and its combinatorial controls. Science. 2010; 329:439–443. [PubMed: 20558669]

Zhang C, Zhang Z, Castle J, Sun S, Johnson J, Krainer AR, Zhang MQ. Defining the regulatory network of the tissue-specific splicing factors Fox-1 and Fox-2. Genes Dev. 2008; 22:2550–2563. [PubMed: 18794351]

Zhou HL, Lou H. Repression of prespliceosome complex formation at two distinct steps by Fox-1/Fox-2 proteins. Mol. Cell. Biol. 2008; 28:5507–5516. [PubMed: 18573872]

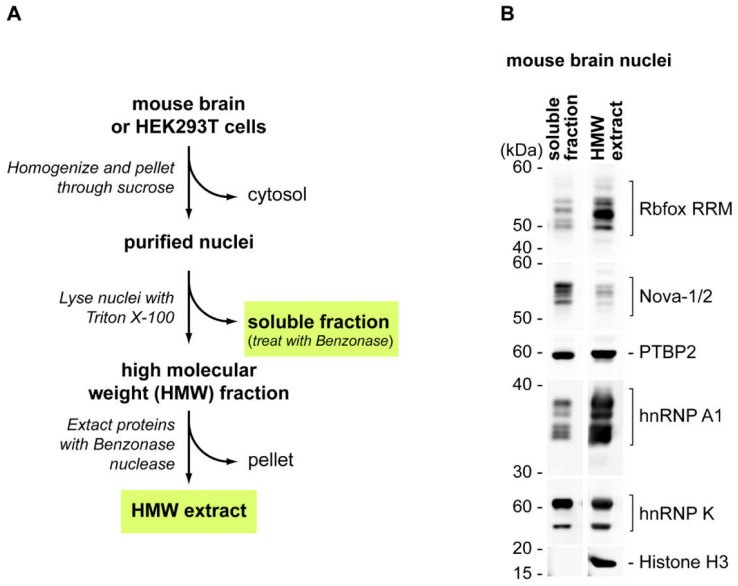

Fig. 1.

Rbfox proteins are found in the high molecular weight nuclear fraction.

(**A**) Preparation of the soluble and HMW nuclear fractions. (**B**) Immunoblot analysis of soluble and HMW fractions from mouse brain. Rbfox1, Rbfox2, and Rbfox3 were detected with an antibody recognizing their nearly identical RRMs.

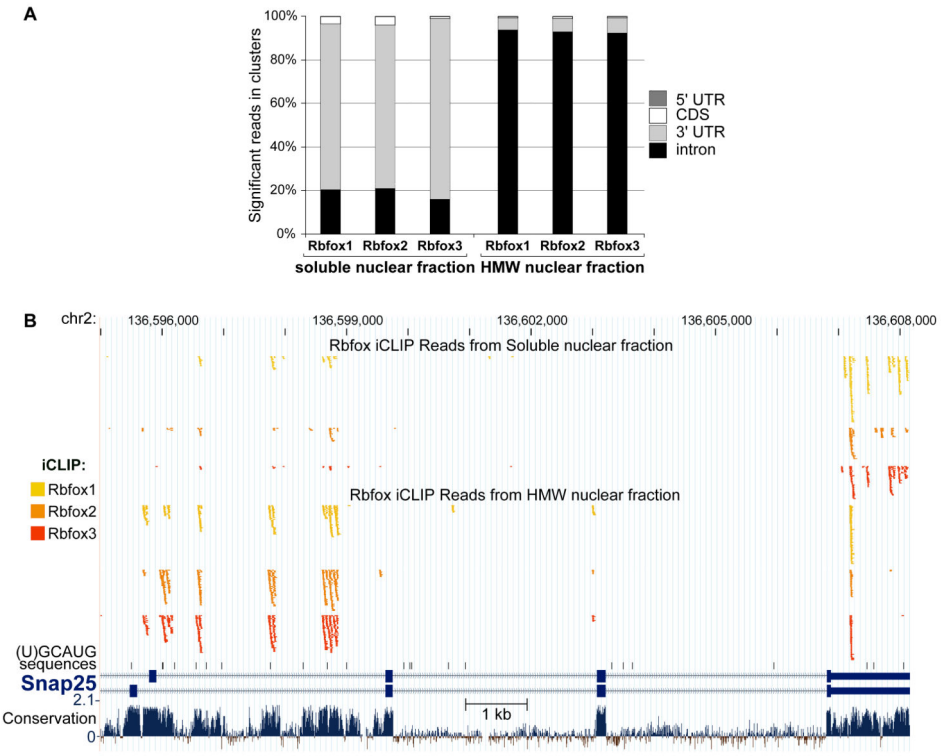

Fig. 2.

Rbfox recruitment to introns in the HMW fraction and to 3′ UTRs in the soluble nuclear fraction.

(**A**) Distribution of Rbfox iCLIP tags in 5′ UTRs, CDS, 3′ UTRs, and introns. Data for mouse brain iCLIP clusters of Rbfox1, 2, and 3 with width ≥2 nt are shown. See Table S1 and Fig. S2 for additional detail. (**B**) Genome browser view of iCLIP reads mapped to the 3′ portion of the Snap25 gene. iCLIP tracks from the soluble nuclear fraction of whole brain and the cerebellar HMW fraction are aligned as indicated. Significant iCLIP reads from Rbfox1, 2, and 3 are colored as indicated. GCAUG motifs are shown below. See Data File S1 for additional examples.

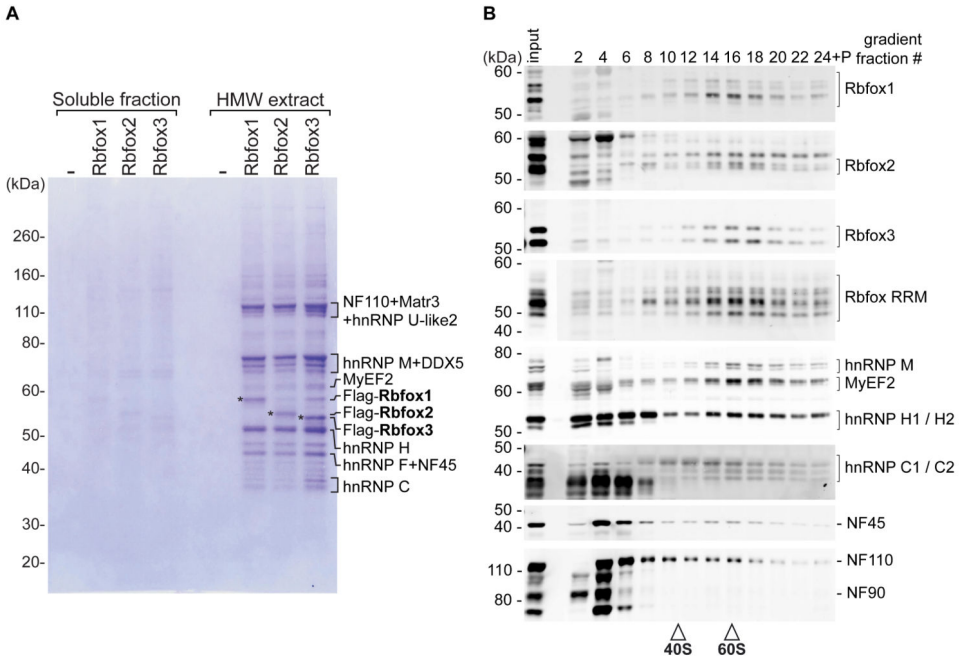

Fig. 3.

Rbfox proteins coprecipitate from the HMW fraction with a distinct set of other RNA binding proteins.

(**A**) Immunopurification of Rbfox proteins from HEK293 nuclear fractions. Soluble and HMW nuclear extracts were prepared from cells stably expressing Flag-tagged Rbfox1, 2, or 3. Proteins were immunoprecipitated with anti-Flag, eluted with Flag peptide, resolved on SDS-PAGE, and stained with SimplyBlue™. The major interacting proteins are indicated on the right. Flag-Rbfox bands are indicated by asterisks. (−) denotes nuclear fractions from the parental HEK293 cell line that does not express Flag-tagged protein.

(**B**) Sedimentation of protein complexes from mouse brain HMW extract through 10-50% glycerol gradients. Gradient fractions from top to bottom run from left to right. 40S and 60S markers from a parallel gradient are indicated below. Rbfox1, Rbfox2, Rbfox3 and their binding partners are indicated on the right. MyEF2 and hnRNP M are detected with common antibody, as are the *ILF3* gene products NF110 and NF90. See Fig. S1 for additional data.

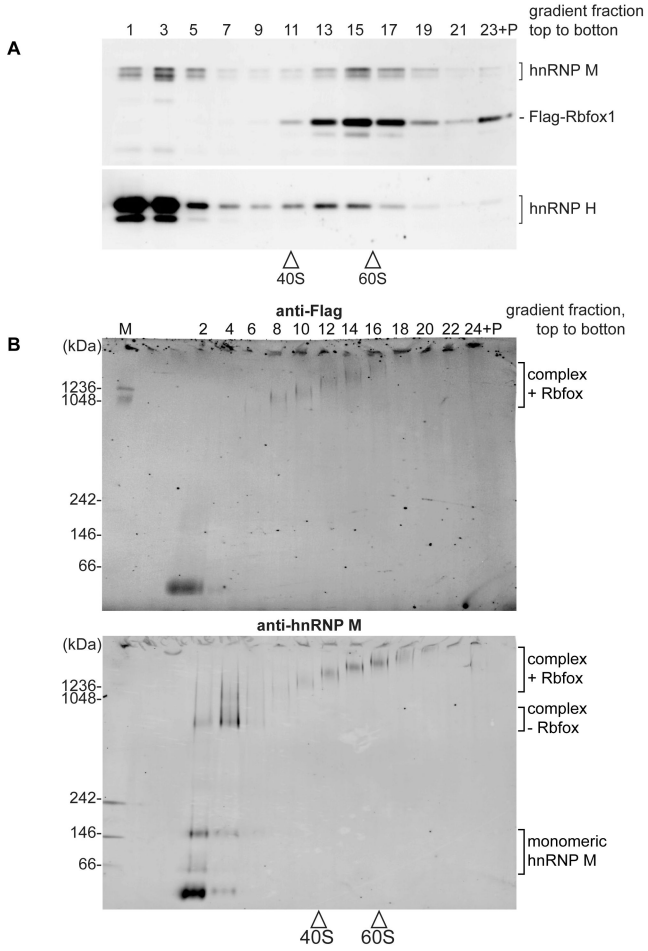

Fig. 4.

The 55S Rbfox complex is present in HEK293 cells and is heterogeneous in size. (**A**) Gradient sedimentation of HMW extract from HEK293T cells transiently expressing Flag-tagged Rbfox1. Proteins detected by immunoblot are indicated as in Fig. 3B. (**B**) Native gel analysis of complexes separated on glycerol gradients. HMW extracts from HEK293 cells stably expressing Flag-tagged Rbfox3 were fractionated and protein complexes were resolved by native PAGE and probed by immunoblot. Flag-Rbfox3 (top) and hnRNP M (bottom) are indicated on the right. See Fig. S3 for further analyses.

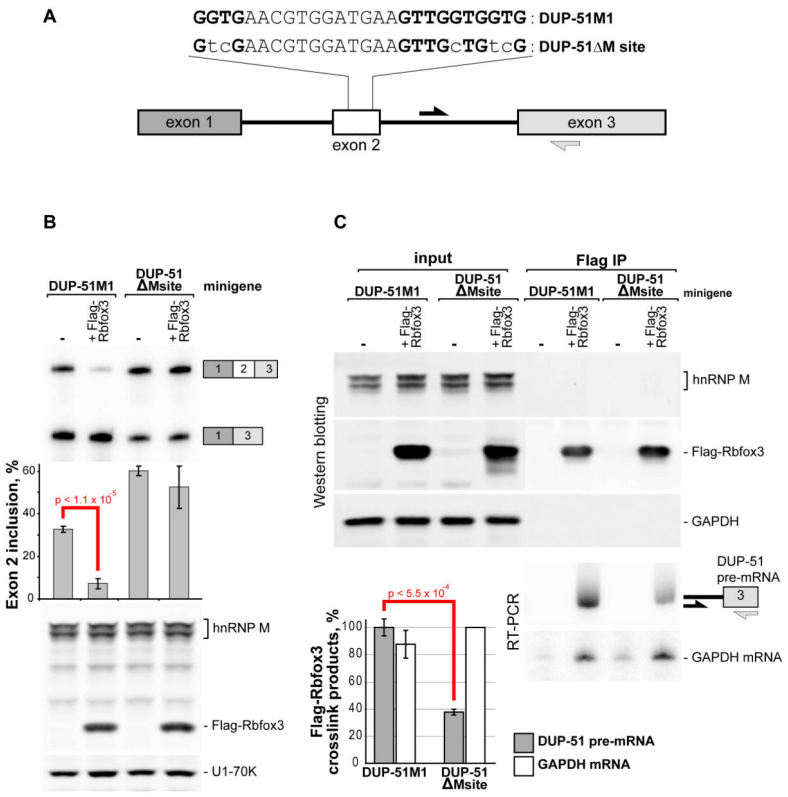

Fig. 5.

Rbfox3 can regulate alternative splicing through an hnRNP M binding site.

(**A**) Diagram of the minigene DUP-51M1 and its mutant DUP-51ΔMsite. The M binding site is in Bold. Arrows indicate primers used to detect DUP-51 premRNA. (**B**) DUP-51M1 or DUP-51ΔMsite were transfected into HEK293T cells with control vector (−) or Flag-Rbfox3 expression vector. Exon 2 splicing was measured by RT-PCR with primers in the flanking exons. The spliced products are indicated (top). Average exon inclusion with standard deviation from four experiments is quantified below. Rbfox3 expression caused a 4.6-fold decrease in DUP-51M1 exon 2 splicing. Statistical significance (red) was measured by unpaired, two-tailed, unequal variance Student's t-test. HnRNP M, Flag-tagged Rbfox3 and U1-70K, as a loading control are indicated (bottom). (**C**) As in B, cells expressing DUP-51 minigenes and Flag-Rbfox3 were UV-irradiated *in vivo* and lysed under denaturing conditions to prevent copurification of hnRNP M. RNA:protein crosslinks were immunoprecipitated with anti-Flag. HnRNP M, Flag-Rbfox3, and GAPDH in the lysates (lanes: input) and immunoprecipitates (lanes: Flag IP) were measured by immunoblot (top). DUP-51 pre-mRNA and GAPDH mRNA were detected by RT-PCR (bottom). Amounts of coprecipitated RNA normalized to the Rbfox3 protein over three experiments are graphed, with means, standard deviation, and p-value as in B. See Fig. S4 and S6 for additional analyses.

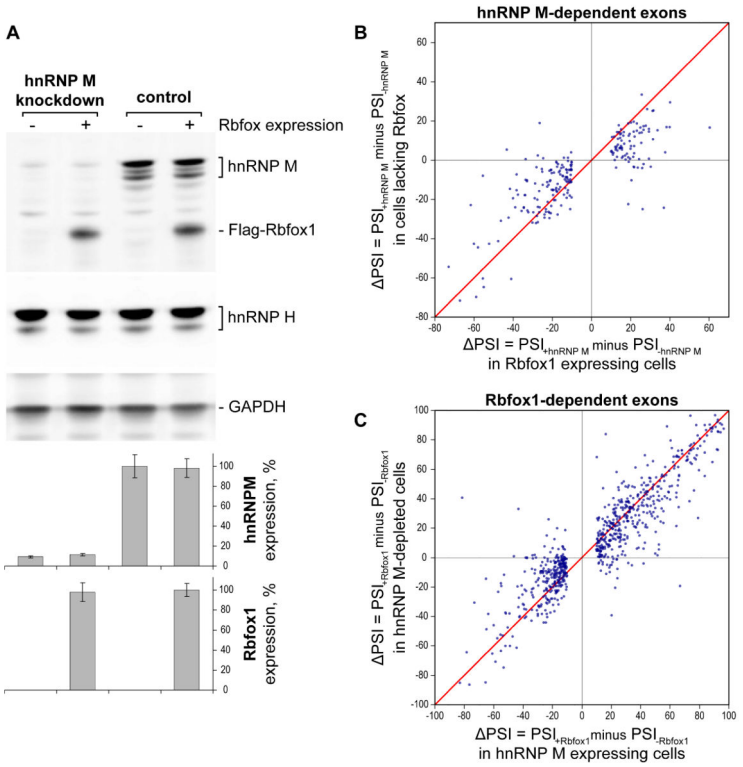

Fig. 6.

Rbfox1 stimulates hnRNP M splicing activity across many exons.

(**A**) Immunoblot of hnRNP M and Rbfox1 in Rbfox2 null HEK293 cells. Rbfox2-knockout cells and derivative cells with Flag-Rbfox1 at the Flp-in locus were grown in doxycycline, transfected with control or hnRNP M-targeted shRNA plasmids and harvested 84 hours post transfection. Relative protein expression over three experiments is graphed below with standard deviation.

(**B**) Comparison of hnRNP M splicing activity in cells expressing Flag-Rbfox1 to that in cells not expressing Rbfox proteins. hnRNP M-regulated exons on this chart were defined in Rbfox1 expressing cells as showing a $|\Delta PSI| > 10$ (PSI in hnRNP M-expressing cells minus PSI in hnRNP M-knockdown cells) and FDR < 0.5. X-axis: ΔPSI values for these exons in Rbfox1 expressing cells. Y axis: corresponding ΔPSI values in Rbfox1-lacking cells.

(**C**) Rbfox1 splicing activity in hnRNP M expressing cells and hnRNP M-depleted cells is compared as in B. See Table S4 for the rMATS analysis.

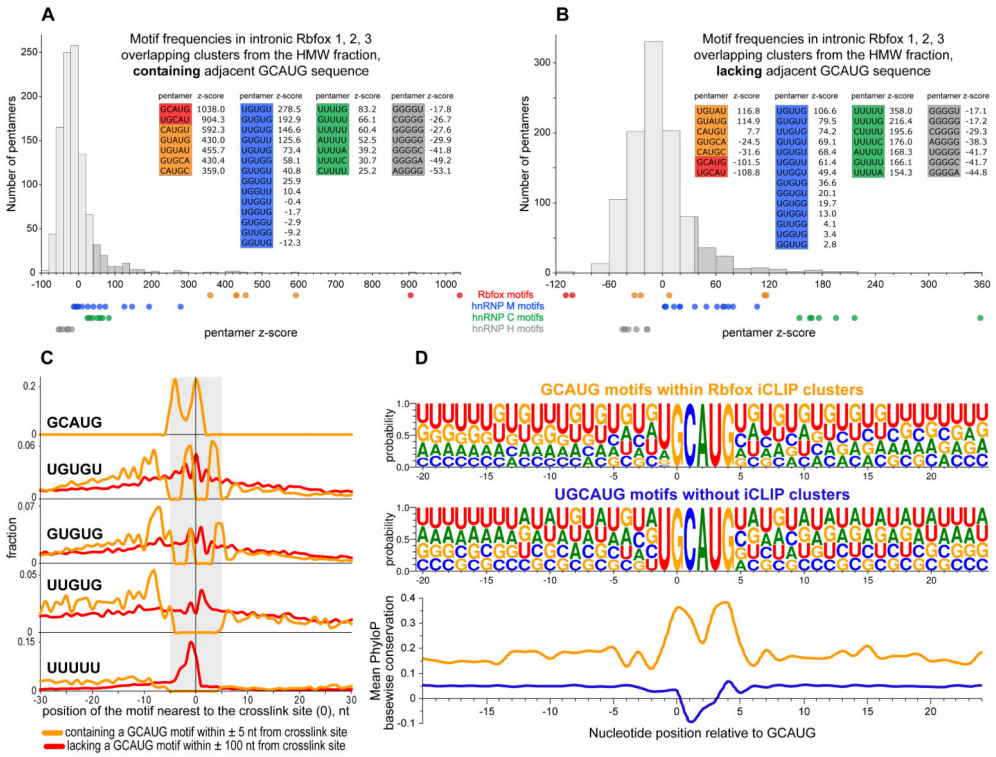

Fig. 7.

Enrichment of sequence motifs near sites of Rbfox binding.

Histogram of pentamer enrichment z-scores within 40 nucleotides of the crosslink sites. iCLIP clusters showing overlap for all three Rbfox paralogs in forebrain or hindbrain HMW fractions were analyzed. Motif enrichments were calculated for crosslink sites less than 40 nucleotides from the nearest GCAUG motif (**A**) or for sites more than 40 nt from this motif (**B**). The top 10 percent of z-scores is shaded darker gray. The Rbfox binding GCAUG, UGCAU (red) and similar pentamers (orange) are indicated as dots below and sorted by z-score above. Motifs recognized by hnRNP M (blue), hnRNP C (green), and hnRNP H (gray) are similarly shown. (**C**) Motif distribution near the crosslink sites. The fraction of sequences with an individual motif aligning at each nucleotide relative to the crosslink site is plotted. Smaller groups of the cluster subsets A and B were analyzed: 1) those containing a GCAUG sequence within 5 nucleotides of the crosslink site (orange lines), and 2) those with a crosslink >100 nt away from the nearest GCAUG (red lines). (**D**) WebLOGO plots of the sequence adjacent to (U)GCAUG motifs (Crooks et al., 2004). Top: Intronic sequences containing a GCAUG motif within 5 nt of an Rbfox crosslink site. Middle: Sequences containing UGCAUG from introns with Rbfox iCLIP clusters, but >100 nt away from the nearest crosslink site. Bottom: Mean PhyloP placental conservation scores of the Weblogo sequences (orange line, crosslinked to Rbfox; blue line, no Rbfox crosslinking). See Fig. S5 for additional information.